# W/SI MULTILAYER GRATINGS FOR X-UV OPTICS

**M. Jergel[1], P. Mikulík[2], E. Majková[1], Š. Luby[1], R. Senderák[1], E. Pinčík[1], M. Brunel[3], P. Hudek[4], I. Kostič[4], A. Konečníková[4]**

[1]*Institute of Physics, Slovak Academy of Sciences, Dúbravská cesta 9, 842 28 Bratislava, Slovakia*
[2]*Laboratory of Thin Films and Nanostructures, Faculty of Science, Masaryk University, Kotlářská 2, 611 37 Brno, Czech Republic*
[3]*Laboratoire de Cristallographie du CNRS, B.P.166, 38042 Grenoble Cedex 09, France*
[4]*Institute of Computer Systems, Slovak Academy of Sciences, Dúbravská cesta 9, 842 37 Bratislava, Slovakia*

## 1. Introduction

X-ray and ultraviolet (X-UV) optics has many applications in plasma source diagnostics, astronomy, projection holography, microscopy, at synchrotron storage rings etc. The main problem is the absence of natural reflective (mirrors) and refractive (lenses) materials in the X-UV region which is due to the fact that absorption is low and that refractive index is less than unity as electronic transitions in atoms start to be excited and resonance effects occur. On the other hand, the latter effect causes a phenomenon of total external reflection (TER) and enables us to design reflection optics working close to the TER region where specular reflectivity is high.

To increase specular reflectivity, periodic multilayers are prepared as artificial structures where not a single surface but many interfaces reflect the incoming beam and under a convenient angle of incidence, the beams reflected from individual interfaces put together in phase to produce an intense specularly reflected beam (Bragg optics). The drawback of planar multilayers is a low spectral resolution. To overcome this problem, laterally structured multilayers with alternating grooves and lamellae (wires), where the reflected X-rays experience Fresnel diffraction (Bragg-Fresnel optics), started to be prepared recently. By shape, they are similar to surface gratings (Fresnel optics) which have been used as monochromators for soft X-ray and UV region long before. Lamellar multilayer gratings (lamellar MLGs, see Fig. 1) combine together a high throughput and a high spectral resolution achieved on higher diffraction orders. A proper structural characterization of a real MLG is a prerequisite to optimize its optical efficiency.

In this paper, we present a structural study of two amorphous periodic lamellar W/Si MLGs, obtained by etching the planar multilayer up to the multilayer substrate, based on scanning-electron microscopy (SEM) observations, X-ray reflectivity (XRR) measurements of coherent grating truncation rods (GTRs) and X-ray diffuse scattering mapping in the reciprocal space. Two different exposure modes to prepare resist mask were examined in these MLGs to optimize the resulting grating structure. The real structural parameters of a more perfect MLG were extracted from fitting the measured GTRs. The XRR simulations are based on the matrix modal eigenvalue approach of the dynamical theory of reflectivity by gratings which generalizes the Fresnel transmission and reflection coefficients for lateral diffraction [1 ,2]. The interface imperfections are taken into account by the coherent amplitude approach which averages the propagation matrices of the wave field over random interface displacements.

Our study has some more general implications for structural characterization of other similarly patterned thin film structures known as mesoscopic structures studied in connection with magnetic, electronic transport, and superconductivity effects.

## 2. Experimental

The planar multilayer was prepared in UMS 500 Balzers apparatus by electron beam evaporation on an oxidized Si(100) wafer with a 0.3 μm thick $SiO_2$ passivation layer. Ten bilayers were deposited at the rate of 0.05 nm/s by alternating deposition of Si (nominal thickness 7 nm) and W (1 nm), Si being the first deposited layer. The layer thickness was controlled by a quartz monitor. The vacuum prior to the deposition $10^{-7}$ Pa decreased to $10^{-6}$ Pa and the substrate temperature increased to 50 °C during the deposition. Further details of the multilayer preparation may be found in [3]. Before further processing, the quality of the planar multilayer was checked by measuring the specular XRR with $CuK_\alpha$ radiation. A multilayer period of (7.8 ± 0.08) nm was found. The internal structure of the individual layers was found to be amorphous by X-ray diffraction. Therefore, any X-ray structural characterization of the MLGs prepared subsequently was confined to the vicinity of the total external reflection (TER) region.

Electron-beam lithography was used to create lamellar grating structure. This patterning method is more universal comparing to optical holography, based on the interference rules, since it enables us to prepare a larger shape variety of patterned structures. Both MLGs were prepared from the same planar multilayer. A 300 nm thick layer of DuPont Elvacite 2041 PMMA resist was spin coated on the multilayer surface. The lithography was performed using a modified ZBA 10/1 direct-write vector-scan pattern generator (Carl Zeiss) with 30 kV accelerating voltage, the minimum spot size and deflection being 25 nm and 50 nm, respectively. The exposure was made by rectangular shots of 5 μm × 300 nm with a base dose of 600 $\mu C/cm^2$, using a combined dose/geometrical proximity correction. A 1 mm × 1 mm periodic array of 1 mm long and 300 nm wide lines was created shot by shot always in one direction (up-down) in one exposure cycle (without moving the sample), the line repetition period being 800 nm. For MLG1, this procedure was done once with a given exposure time. For

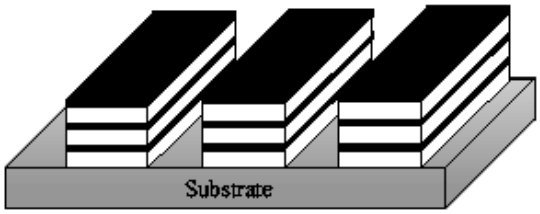


**Fig. 1.** Schematical view of a MLG with the wire width to period ratio $\Gamma = 0.625$ and individual layer thicknesses ratio $t_A/t_B = 7$ which are the nominal values of the MLGs under study. To simplify the drawing, only 3 periods are shown instead of 10.

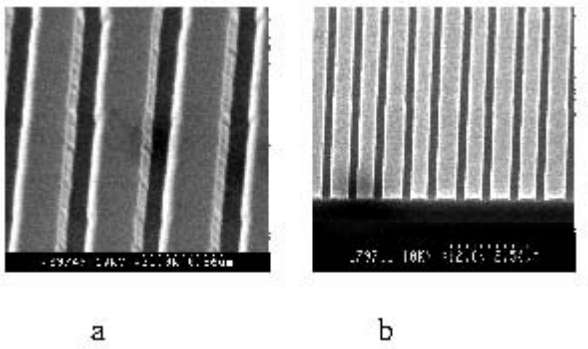


**Fig. 2**. SEM photographs of the MLG1- top view (a) and side view (cross-section - b) which show a real grating shape.

MLG2, this procedure was done twice with a half exposure time each, the connecting points of the rectangular spots 5 μm × 300 nm along the line being shifted at the second exposure. The motivation was to suppress local heating effects [4] and to obtain smoother walls of the grooves. For each MLG, a resulting resist mask of the total area 5 mm × 5 mm corresponding to a grating with the wire width and lateral period of 500 nm and 800 nm (1250 wires/mm), respectively, was achieved by sequential repositioning the sample. The final grating structure was obtained by $Ar^+$ ion beam etching (LPA USI Model Ionic) across the whole multilayer up to the substrate kept at 15 °C with a current density of 0.35 mA/cm$^2$ in a vacuum of $10^{-3}$ Pa. The residual resist was removed by standard wet and dry procedures.

The prepared MLGs were inspected by atomic force microscopy and scanning electron microscopy (low-voltage field-emission Hitachi S 800). The XRR measurements were done on a laboratory-made four-circle diffractometer. $CuK_\alpha$ radiation provided by a Rigaku 12 kW rotating anode generator was monochromatized by a graphite monochromator and limited to a 50 μm wide beam by a slit. A NaI(Tl) scintillation detector was used with a slit of 80 μm.

## 3. Results and discussion

The AFM and SEM pictures revealed a fairly regular grating shape with the lateral period close to the nominal one. An example of the SEM pictures from MLG1 is shown in Fig. 2. A similar quality of the grating shape was achieved on MLG2.

Firstly, specular GTR (GTR of zero order, Fig. 3) and scans (rocking scans) with the detector positioned at different ML Bragg orders were measured. The scans around the 2nd Bragg order for both MLGs are shown in Fig. 4. In addition to the specular peak in the center, additional peaks are superimposed on a broad background coming from the diffuse scattering by rough interfaces. The largest side peaks are the intersections of the scan trajectory in the reciprocal space with the GTRs. A GTR of order $m$ is cut at (so-called *grating rule*)

$$m\lambda = d(\cos\theta_2 - \cos\omega) \qquad (1)$$

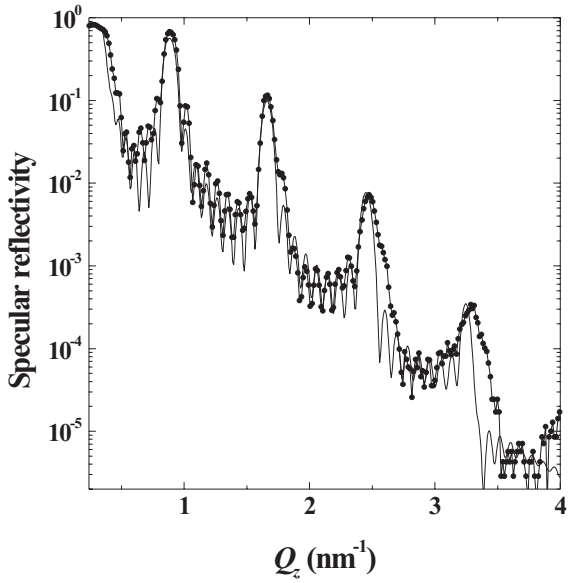


**Fig. 3.** Measurement (thin line with points) and fit (thick line) of the specular GTR as a function of the normal (perpendicular to the interfaces) wave vector transfer $Q_z$ for MLG1. Angle of incidence of the measurement ranged from 0.15° to 3°.

for the angles of incidence and exit $\omega$ and $\theta_2$, respectively, which gives the lateral period of our MLGs $d$ = 780 nm. The smaller peaks in the ω scans between the large ones correspond to a multiple lateral period, namely double (MLG1) and triple (MLG2), their intensity being by one order of magnitude lower. On closer inspection of the cross-section SEM photograph (Fig. 2 b), it may be seen that every second wire is slightly narrower (by less than ≈ 5%) and causes a lateral superperiodicity stretching on a MLG area large enough to produce visible effects. A similar effect is observable on MLG2 where two broader wires alternate with a narrower one. These MLG features are caused by secondary effects of the patterning procedure like local heating effect which was not suppressed in MLG2 as expected. Moreover, a stitching accuracy of the 1 mm × 1 mm arrays exposed at fixed sample positions was kept below 100 nm for MLG1 but was worse for MLG2. Therefore, MLG1 was chosen for a more detailed study.

The GTRs of MLG1 are directly visible in the measured reciprocal space map of the scattered intensity (Fig. 5). Furthermore, we can see the clouds of more intense dif-

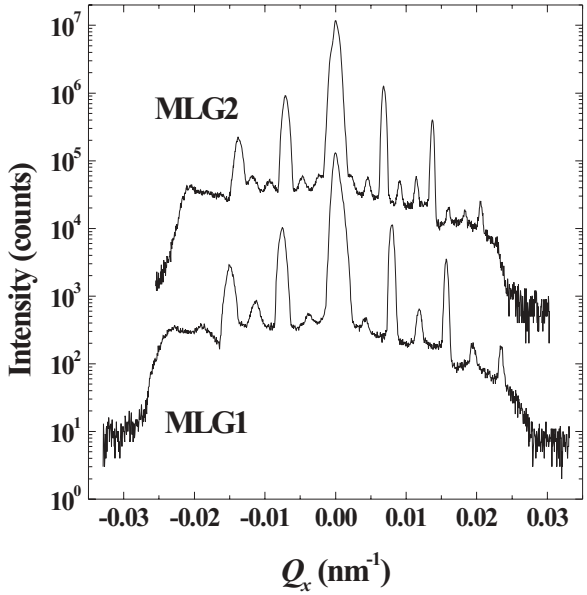


**Fig. 4.** ω scans measured on MLG1 and MLG2 with the detector positioned at the 2nd Bragg order (2θ =2.33°) as a function of the lateral (along the interfaces) wave vector transfer $Q_x$. The curve for MLG2 is shifted upwards by the factor of $10^2$.

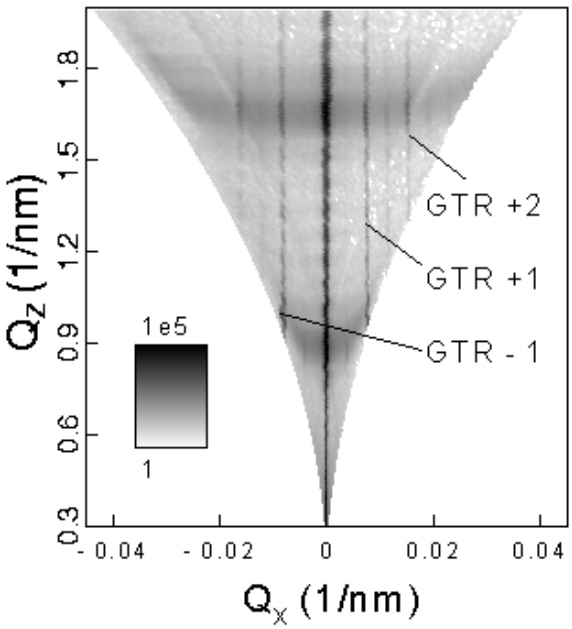


**Fig. 5**. Measured reciprocal space map of the scattered intensity for MLG1.

fuse scattering around the ML Bragg peaks which give evidence of the roughness correlated from one interface to another [5].

Finally, the GTRs of MLG1 of non-zero orders were measured separately with the sample and detector moving according to the *grating rule* mode. Some of them (together with their fits) are shown in Fig. 6. We note that the $Q_z$ profiles of the GTRs of opposite orders were found equal (withing the experimental precision) which complies with the theoretical prediction for scattering without strong dynamical effects [2].

For the quantitative analysis, the GTRs were fitted using the dynamical theory for rough multilayer gratings [1,2]. We noticed that for the given wavelength and grating period, no multiple scattering effects are distinguishable in the specular GTR so that this one could be fitted by usual algorithms for averaged planar multilayers. The multilayer Bragg peak positions determined the multilayer period $t$ = (7.73 ± 0.07) nm which compares well with $t$ = (7.8 ± 0.08) nm determined before patterning. The presence of only 7 multilayer thickness oscillations instead of 8 between two subsequent Bragg peaks in GTRs, unlike the ML specular XRR curve measured before patterning, points to a reduction of the uppermost period. This reduction is due to an oxidized tungsten layer which is naturally formed at the multilayer surface in the air. This layer was mechanically removed by plasma ions and/or thermally evaporated during the oxygen plasma treatment which was applied in the last step of the cleaning procedure. This step was inevitable to remove the resist also from the MLG grooves. It is known that tungsten oxides have a low mechanical compatibility and some of them are volatile at elevated temperatures [6].

The maximum position of the transmission function of the incident wave penetrating into the multilayer, represented by the critical angle for TER on the specular GTR and by the first sharp peak on other GTRs, depends on the average density of the sample. According to single-scattering theories for gratings, like the kinematical theory and the DWBA [2,7], the most remarkable effect of the wire width to period ratio Γ is the modulation of the intensity of GTRs of different order at constant $Q_z$. The ratio of the Si and W layer thicknesses and interface roughness influence the modulation of the intensity profile along each GTR. The wire width to period ratio was determined as Γ = (0.7 ± 0.08) and the individual layer thicknesses as $t_{Si}$ = (6.23 ± 0.07) nm and $t_w$ = (1.5 ± 0.07) nm, the reduced

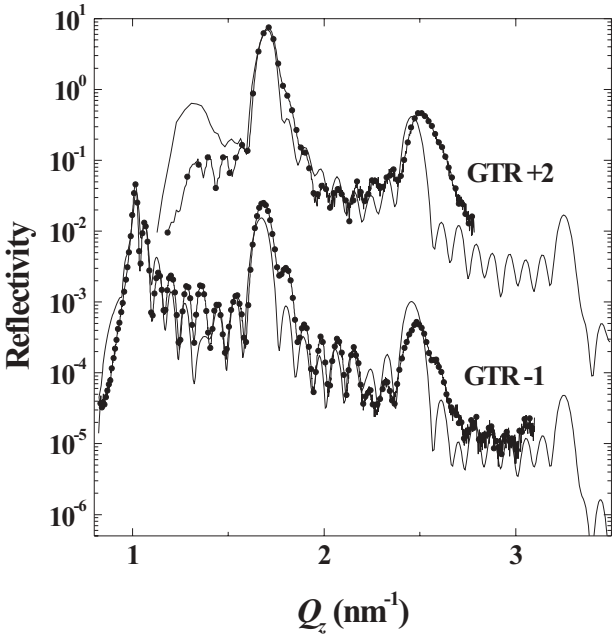


**Fig. 6.** Measurements (thin lines with points) and fits (thick lines) of the GTR -1 and GTR +2 as a function of the normal wave vector transfer $Q_z$ for MLG1 (angle of incidence during the measurements ranged from 0.03° to 2.03° and from 1.61° to 2.29°, respectively). Curve GTR +2 is shifted upwards by the factor of $10^3$.

thickness of the uppermost W layer discussed above being (0.43 ± 0.3) nm. The interface and surface roughness values are (0.58 ± 0.05) nm and (0.43 ± 0.07) nm, respectively. The obtained set of fitted parameters is mutually consistent for all treated GTRs.

The side wall roughness observable on the SEM photographs (Fig. 2a) is estimated to be below 50 nm. Such small side wall fluctuations do not influence the intensity of low-order GTRs since the lateral wave vector transfer $Q_x$ is large [2], contrary to the high sensitivity to interface roughness which is of the same order as $1/Q_z$, $Q_z$ being the normal wave vector transfer. The above-mentioned effect of the lateral superperiodicity could be simulated by involving a double period in the dynamical calculation and reevaluating the Fourier coefficients of susceptibility for wires with two different widths. However, this effect, being subtle, did not affect the measured GTRs of the first two orders substantially.

## 4. Conclusions

Two lamellar multilayer gratings with the nominal normal and lateral periods 8 nm and 800 nm, respectively, were obtained by etching a planar amorphous W/Si multilayer up to the substrate. An exposure mode for the preparation of the MLG resist mask giving better results was specified. The atomic force microscopy and scanning electron microscopy revealed a fairly regular grating shape while the XRR measurements enabled us to examine the inner part of the MLGs. The specular reflectivity, GTRs of non-zero orders, and a reciprocal space map of the scattered intensity close to the total external reflection were measured using the $CuK_\alpha$ radiation. We demonstrated a possibility of extracting real structural parameters, such as the layer set-up, interface roughness and wire width to period ratio, of a fully etched periodic MLG from fitting the measured truncation rods.

**Acknowledgements**

*This work was partly supported by the Slovak Grant Agency (VEGA), project No. 5083/98, and Ministry of Education of the Czech Republic, project No. VS 96 102.*

## References

1. P. Mikulík & T. Baumbach, *Phys. Rev. B*., **59** (1999), 7632-7643
2. P. Mikulík: X-ray reflectivity from planar and structured multilayers. PhD thesis, Université J. Fourier (Grenoble) and Masaryk University (Brno) 1997.
3. Š. Luby, E. Majková, P. Lobotka, I. Vávra, M. Jergel, R. Senderák, & J. Grňo, *Physica*, **C 197** (1992) 35-41.
4. S. Babin, P. Hudek & I. Kostič, *J. Vac. Sci. Technol.*, **B 15** (1997) 311-318.
5. V. Holý & T. Baumbach, *Phys. Rev.*, **B 49** (1994) 10668-10676.
6. J.W. Mellor: A Comprehensive Treatise on Inorganic and Theoretical Chemistry, Vol. XI. London-NewYork-Toronto 1931. Longmans, Green and Co. p. 753.
7. P. Mikulík & T. Baumbach, *Physica B*, **248** (1998), 381-386